

Application Note #1542

Time-Dependent Plasticity in High-Temperature Pillar Compression

Structural materials in demanding applications can be subject both to high stresses and high temperatures simultaneously. The combination of stress and temperature in metals often leads to time-dependent plastic responses, or creep, which can easily lead to premature failure. Creep at temperature is commonly studied with bulk scale specimens, but can also be done at the microscale. In-situ SEM micro-pillar compression allows specific regions of the microstructure, such as individual grains, to be targeted and allows for high-resolution characterization of the deformation mechanisms. A variety of load functions can be employed to characterize the time-dependent response: load relaxation, creep, or strain rate jump tests. The data from these can be used to fit activation volumes and energies, which indicate the dominant dislocation processes. In this way, incredibly detailed deformation process maps, as a function of temperature, stress, strain rate, and grain orientation, can be envisioned. This would aid in optimizing current- and next-generation materials design. This application discusses in-situ SEM micro-pillar compression tests of a Ni-based superalloy, IN718, at 650°C tested with three types of load functions designed to probe the time-dependent response. These include a linear quasistatic loading, a stress relaxation test,¹ and a strain rate jump test.² The use of in-situ SEM has additional synergy with the high-temperature testing, as the high vacuum of the SEM helps protect the material from oxidation during testing.

Experimental Procedure

A Hysitron PI 89 SEM PicoIndenter equipped with the 800°C heating option and a 10-micron diamond flat punch tip was utilized to perform the testing. The superalloy sample comes from Raytheon Technologies Research Center.* The pillars, fabricated via focused ion beam, were machined into a single grain as confirmed by electron backscatter diffraction (EBSD). The sample mounted on the heating stage is shown in Figure 1, along with the locations of the three test pillars and their load functions. These pillars were approximately 10 microns tall and 5 microns in diameter. The sample and tip were heated to 650°C at a rate of 30°C per minute. The load function for each pillar is described alongside the results. Stress and strain calculations were facilitated by using the Tribo iQ analysis application, which can also generate side-by-side stress-strain videos with the SEM videos. A Sneddon correction was also applied to compensate for the pillar pushing into the substrate.

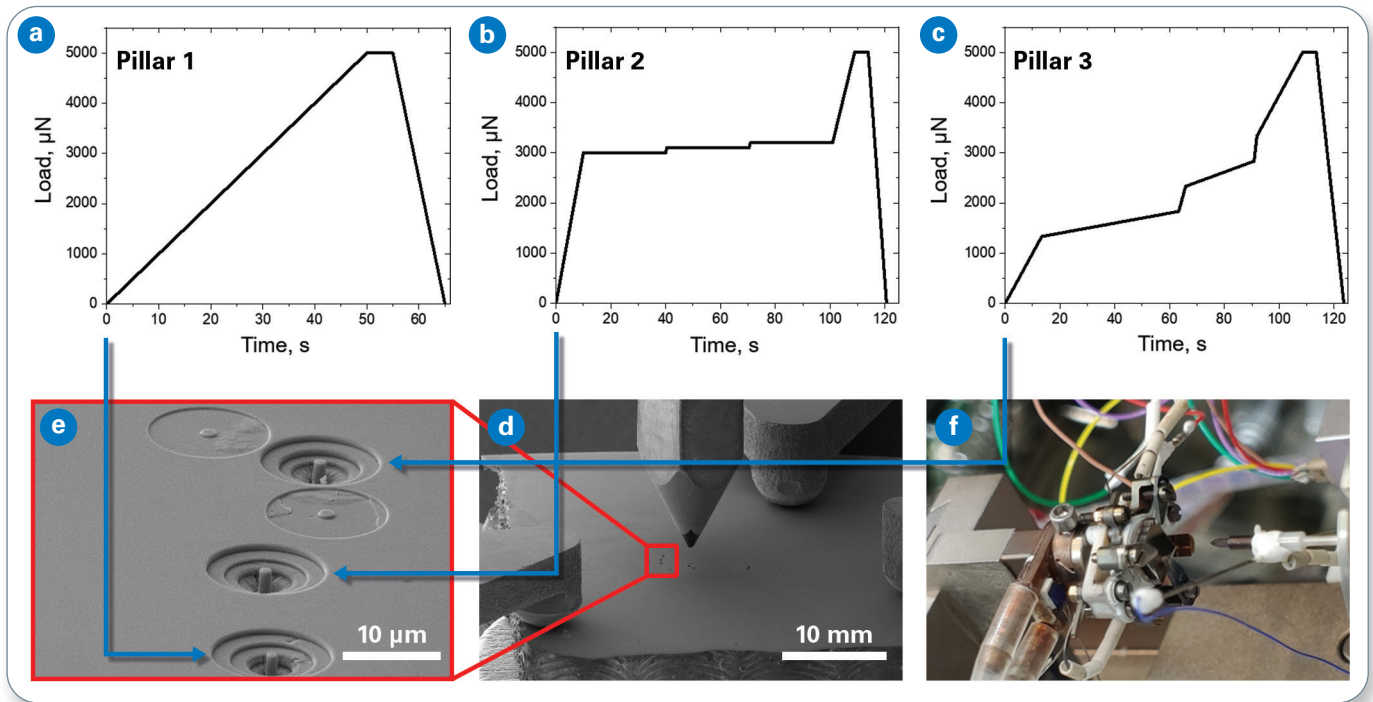


Figure 1. Overview of the experiments: (a-c) three different load functions are applied to (d) each of three pillars, with the sample clamped to the sample heater shown in (e) and (f).

Results and Discussion

The results for Pillar 1 are shown in Figure 2, which was subjected to linear quasistatic loading. Loading time is set to 50 seconds with a rate of 100 nanometers per second, with a 5-second hold and 10-second unload. As can be observed, oxide is flaking off the outside of the pillar during the test, even with the protective environment of the SEM vacuum. The presence of an oxide can alter the image forces acting

on dislocations and potentially provide some confining stress. Overall, the stress-strain response is characteristic of a metal, with a linear elastic slope up to the yield point, where the load-displacement curve curls over. After the yield point, sporadic large load drops occurred, which were correlated to the formation of slip steps on the surface with little to no strain hardening. The slip appears to be multi-slip based upon the post-test image.

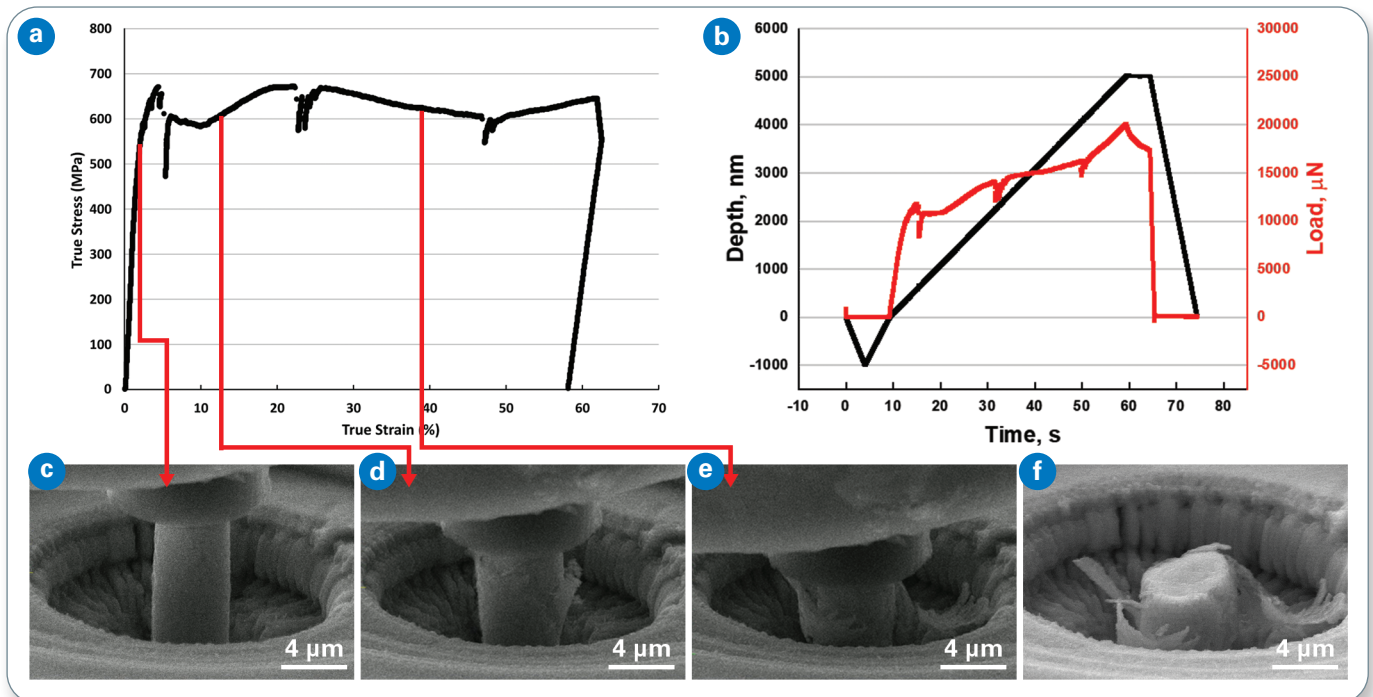


Figure 2. (a) True stress versus true strain, and (b) load and displacement versus time for Pillar 1. Frames from the in-situ video are also shown (c-f). This pillar was subjected to a linear quasistatic loading under displacement control.

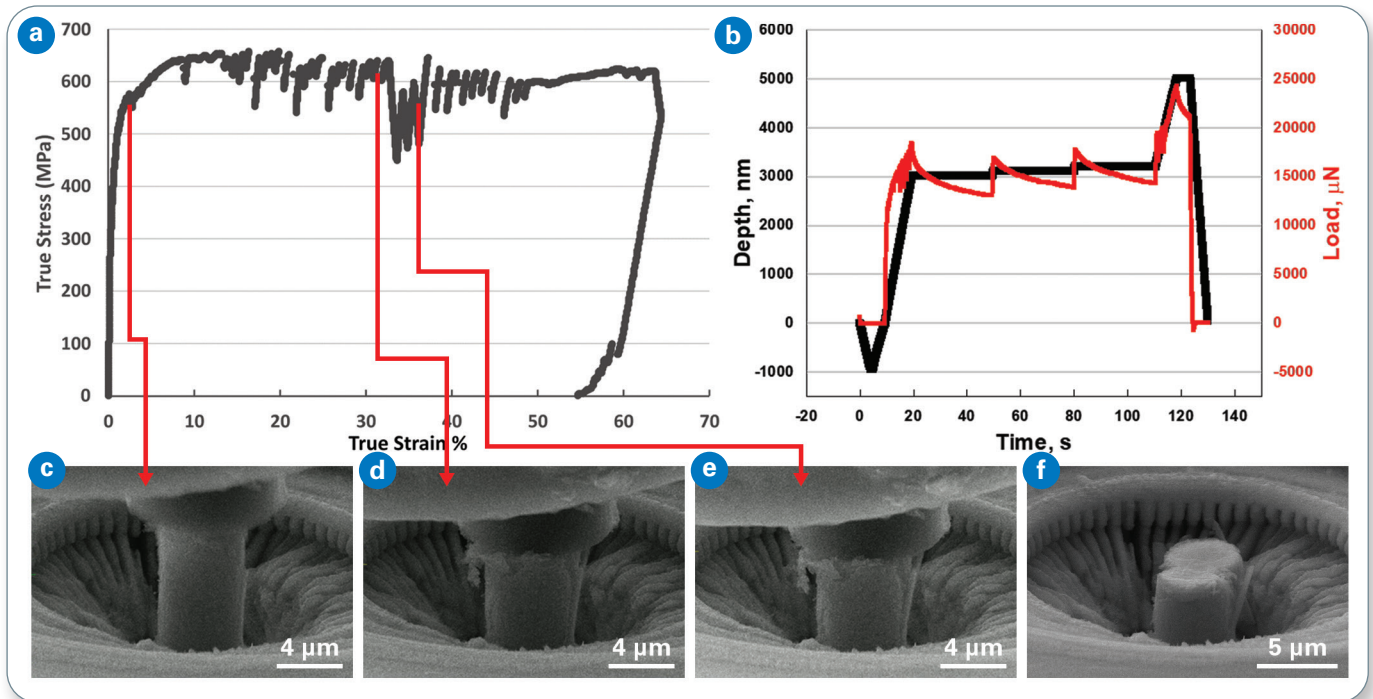


Figure 3. (a) True stress versus true strain, and (b) load and displacement versus time for Pillar 2. Frames from the in-situ video are also shown (c-f). This pillar was subjected to three load relaxation holds, where the displacement was held constant in displacement control after plasticity was induced.

Figure 3 shows the results from Pillar 2. This was subjected to three load relaxations, which were performed well into the plastic regime. Three separate load relaxations of 30-second duration were employed, starting at 60% of the prescribed displacement to ensure they occur in the plastic regime. Due to relaxation, a small amount of reloading is required between cycles, which was set to 100 nanometers. The overall stress-strain response was similar to that of Pillar 1, however, the load relaxations show some details of the time-dependent plastic response in the

pillar. At elevated temperatures, thermal energy provides additional mechanism for dislocations to maneuver around any unspecified obstacles by cross-slip or climb. Each load relaxation event appears to have a slightly lower slope than the previous one, as expected due to the constantly decreasing density of stored dislocations versus time. Initially upon reloading, the relaxation rate is slightly higher than the end point of the previous cycle, indicating that some additional dislocations are introduced upon reload.

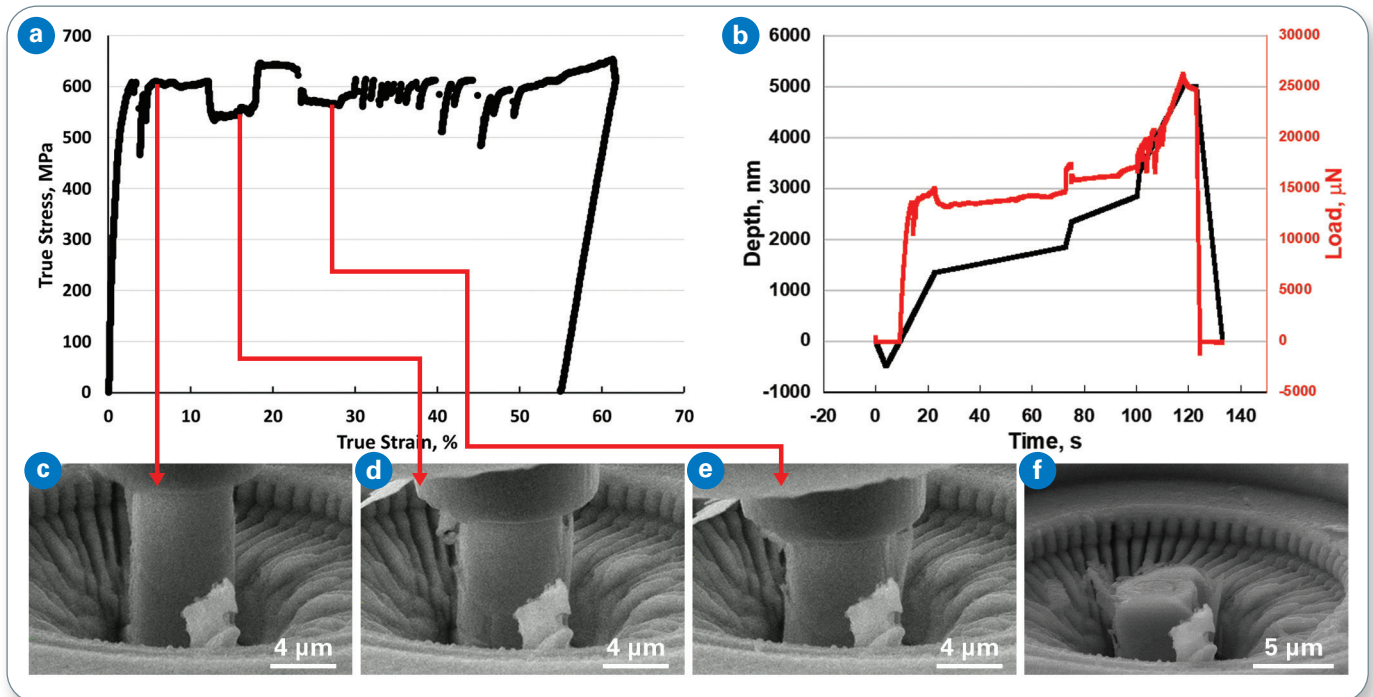


Figure 4. (a) True stress versus true strain, and (b) load and displacement versus time for Pillar 3. Frames from the in-situ video are also shown (c-f). This pillar was subjected to strain rate jump tests, consisting of 5 jumps over 1.5 orders of magnitude.

Figure 4 shows the results from Pillar 3. This pillar was subjected to strain rate jumps using displacement control. The strain rate jump test had five jumps covering 1.5 orders of magnitude in strain rate (strain rates of $0.007s^{-1}$, $0.0007s^{-1}$, $0.014s^{-1}$, $0.0014s^{-1}$, $0.07s^{-1}$ corresponded to displacement rates of 100 nm/s, 10 nm/s, 200 nm/s, 20 nm/s, 500 nm/s). Again, the overall stress-strain curve is similar to Pillar 1 and Pillar 2, but the details occurring during the strain rate jumps are indicative of time-dependent plastic response. It can be observed that higher stresses are required for higher loading rates, as expected. The amount of stress change between each strain rate can be utilized to determine stress versus strain rate, the fit of which is related to the activation volume.

The stress strain and load-displacement response of all three pillars are compared in Figure 5. The responses are similar, giving a yield stress between 500 and 700 MPa at this temperature.

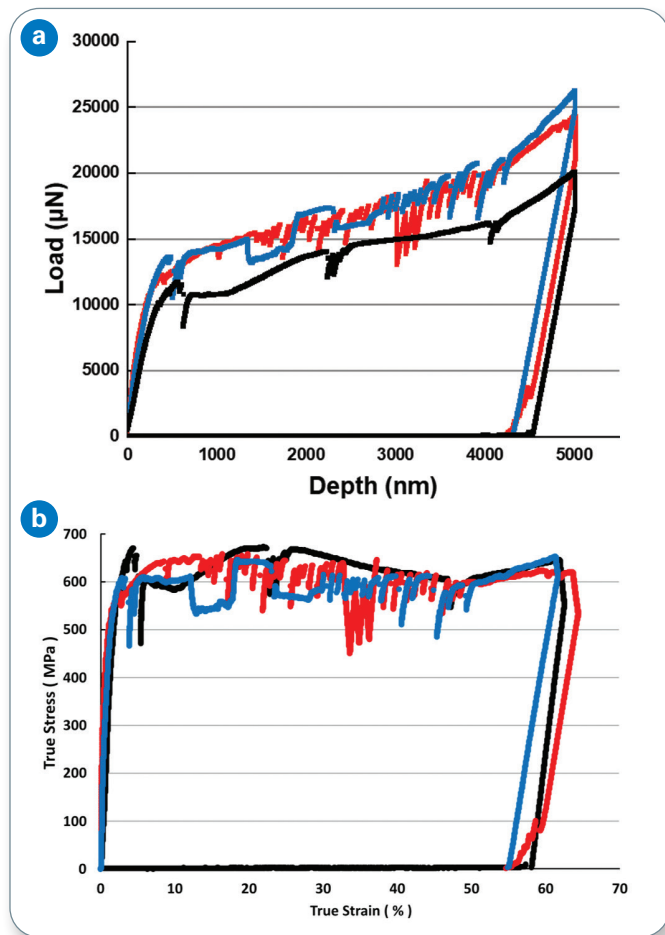


Figure 5. Comparison of (a) load-displacement and (b) true stress versus true strain curves for the three pillars.

Conclusions

The three types of load function were successfully employed at 650°C to each of the three superalloy pillars. The overall stress-strain response was similar, but the use of strain rate jumps on Pillar 3, and load relaxations in Pillar 2 provide insight into the time-dependent plastic response. At elevated temperatures, substantial relaxation and strain rate sensitivity were observed, indicating prevalent thermally activated dislocation motion mechanisms. The results also show that the Hysitron PI 89 SEM PicoIndenter is an ideal means of investigating deformation mechanisms at high resolution.

References

1. Yan, Y., Chen, W., Sumigawa, T., Wang, X., Kitamura, T. and Xuan, F.Z., 2020. A Quantitative In Situ SEM Bending Method for Stress Relaxation of Microscale Materials at Room Temperature. *Experimental Mechanics*, 60(7), pp.937-947.
2. Snel, J., Monclús, M.A., Castillo-Rodriguez, M., Mara, N., Beyerlein, I.J., Llorca, J. and Molina-Aldareguia, J.M., 2017. Deformation mechanism map of Cu/Nb nanoscale metallic multilayers as a function of temperature and layer thickness. *JOM*, 69(11), pp.2214-2226.

*Acknowledgment: The material from RTRC is based upon work supported by the Department of Energy under Award Number(s) DE-FE0031642.

Disclaimer: "This report was prepared as an account of work sponsored by an agency of the United States Government. Neither the United States Government nor any agency thereof, nor any of their employees, makes any warranty, express or implied, or assumes any legal liability or responsibility for the accuracy, completeness, or usefulness of any information, apparatus, product, or process disclosed, or represents that its use would not infringe privately owned rights. Reference herein to any specific commercial product, process, or service by trade name, trademark, manufacturer, or otherwise does not necessarily constitute or imply its endorsement, recommendation, or favoring by the United States Government or any agency thereof. The views and opinions of authors expressed herein do not necessarily state or reflect those of the United States Government or any agency thereof."

● Bruker Nano Surfaces and Metrology Division

Minneapolis, MN · USA

+1.952.835.6366

productinfo@bruker.com

www.bruker.com/picoindenters